This full text paper was peer reviewed at the direction of IEEE Communications Society subject matter experts for publication in the IEEE ICC 2011 proceedings

Design of Distributed Multi-Edge Type LDPC Codes for Two-Way Relay Channels

Marwan H. Azmi, Jun Li, Jinhong Yuan and Robert Malaney

School of Electrical Engineering and Telecommunications
University of New South Wales, Sydney, NSW 2052, AUSTRALIA
Email: marwan@student.unsw.edu.au, jun.li@unsw.edu.au, j.yuan@unsw.edu.au, r.malaney@unsw.edu.au

***Abstract*— This paper studies the problem of finding the optimum degree distribution for the distributed LDPC codes in the two-way relay channels. Based on the framework of multi-edge type (MET) LDPC codes, we propose a methodology to asymptotically optimize the code's ensemble when different segments within the distributed codeword have been transmitted through different channels and experience different SNRs. An average noise threshold is formulated to compute the convergence threshold of the distributed LDPC codes under density evolution and acts as the performance gap between the optimized distributed codes and the theoretical limit. We demonstrate that the optimized distributed LDPC code using our proposed method performs asymptotically within a fraction of a dB away from the theoretical limit.**

I. INTRODUCTION

The concept of network coding, proposed by Ahlswede, Cai, Li and Yeung in [1], increases the achievable throughput in a network. A network utilizing this concept that has attracted much research interest is the two-way relay channel (TWRC). In a two-way relay communication, two users want to exchange their independent messages with the help of a common relay. The fundamental limit for TWRC has been studied in [2], [3], [4]. In addition, a network and channel code design based on the idea of distributed turbo codes has been proposed in TWRC [5]. The work in [6] extends the distributed turbo code design to the asymmetric TWRC.

Low-density parity-check (LDPC) codes have been shown to be a class of powerful codes with superior capacity-achieving performance [7]. However, there is no reported work regarding the design of capacity-achieving distributed LDPC codes in TWRC. The structure of distributed LDPC codes is different from the structure of bilayer LDPC codes [8], as the additional parity bits of the distributed LDPC codes generated by the relay are broadcasted without a protection from relay's codebook, i.e. the channel between the relay and the intended receiver is not error free. As a result, the entire distributed LDPC codeword consists of the original LDPC codeword (mother codeword) sent by the transmitter and the additional parity bits generated by the relay. The parity check matrix to decode the distributed LDPC codes at the intended receiver is similar to the rate-compatible LDPC codes under a framework of automatic repeat request/forward error correction (ARQ/FEC) protocols [9]. However, there is a significant fundamental difference between the codes in these two frameworks (applications). In the distributed LDPC codes, the received additional (incremental) parity bits at the receiver have undergo different channel (relay-to-receiver) and experience different signal-to-noise ratio (SNR) than the received bits in the mother code.

This paper extends the general concept of irregular LDPC codes, introduced by multi-edge type (MET) LDPC codes, to the construction of distributed LDPC codes for time-division TWRC. A new design technique for the distributed LDPC codes is proposed as different segments within the distributed codeword have been transmitted through different channels and experience different SNRs. An average noise threshold is formulated to compute the convergence threshold of the distributed LDPC codes under density evolution. We demonstrate that the optimized distributed LDPC code using our proposed method performs asymptotically within a fraction of a dB away from the theoretical limit.

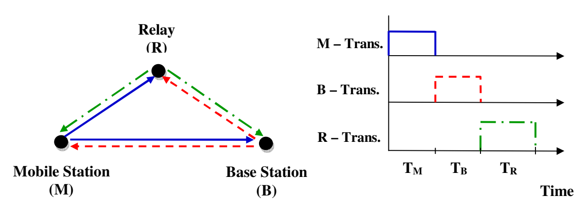

Fig. 1. Time-division two-way relay channels.

II. SYSTEM MODEL

We consider cooperative uplink and downlink channels between mobile and base stations with the help of one common half-duplex relay (R). Here, the mobile station (M) and the base station (B) want to exchange independent messages. This channel can be modeled as the time-division (TD) two-way relay channel depicted in Fig. 1, with broadcast transmissions at all nodes. The transmitted power at all nodes is equal and given by P. The system's transmission takes place in three phases. In the first phase, M broadcasts to B and R. In the second phase, B broadcasts to M and R. In the third phase, R broadcasts to M and B. The normalized period of transmission in all phases is given by $T_M + T_B + T_R = 1$. In one normalized period of transmission, N symbols are transmitted, i.e. M, B and R broadcast $N_M = T_M \cdot N$, $N_B = T_B \cdot N$ and

$N_R = T_R \cdot N$ symbols, respectively. The received signals at any node in TD-TWRC are defined by

$$Y_{kl} = \frac{1}{\sqrt{d_{kl}^{\alpha}}} X_k + Z_{kl} \quad (1)$$

for $k, l \in \{M, R, B\}$ and $k \neq l$. Y_{kl} denotes the received signal at node *l* transmitted from node *k*, while X_k denotes the transmitted signals from node k. The corresponding distance between node k and node l is d_{kl}. The noise value Z_{kl} at node l is zero-mean and unit variance Gaussian. Thus, the received SNR between two nodes is $\gamma_{kl} = P/(d_{kl}^{\alpha})$, with α denotes the path-loss exponent. In this work, we restricted our attention to Gaussian two-way relay channel at low SNR for which binary linear codes are near optimum and binary phase shift keying (BPSK) modulation is applied in the transmission. We denote $C(\gamma)$ as the capacity for the binary additive white Gaussian noise (BAWGN) channel.

For a symmetric-topology where $d_{MR} = d_{BR}$, the uplink and downlink capacities are equal since $C(\gamma_{MR}) = C(\gamma_{BR})$. If $C(\gamma_{MB}) \leq 2 \cdot C(\gamma_{BR})$, the optimal value of time sharing parameter for M (uplink) and B (downlink) that maximizes the total transmission rate is given by [10]

$$T_M^* = T_B^* = \frac{C(\gamma_{RB})}{C(\gamma_{MR}) + 2 \cdot C(\gamma_{RB}) - C(\gamma_{MB})}. \quad (2)$$

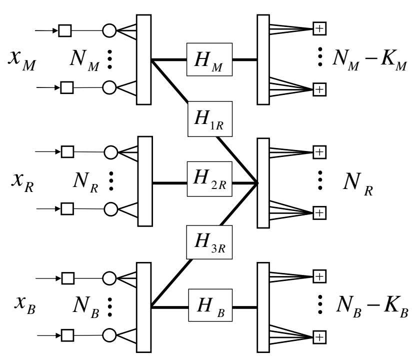

Fig. 2. The distributed LDPC codes for time-division two-way relay channels.

III. LDPC CODING FOR TWRC

In this section, we explain how to realize joint network-channel coding for TD-TWRC based on LDPC codes. We define K_M and K_B as the number of independent messages (bits) that M and B want to exchange.

A. Channel encoding

In the first phase, M encodes K_M information bits into an LDPC code denoted by vector $\mathbf{X}_M$ of length N_M. To ensure a successful decoding of $\mathbf{X}_M$ at R, the designed rate for $\mathbf{X}_M$ must satisfy

$$R_{MR} = \frac{K_M}{N_M} \leq C(\gamma_{MR}). \quad (3)$$

In the second phase, another LDPC code denoted by vector $\mathbf{X}_B$ of length N_B is generated by B in order to protect and forward K_B information bits to M and R. In this transmission, a successful decoding of $\mathbf{X}_B$ at R is guaranteed if

$$R_{BR} = \frac{K_B}{N_B} \leq C(\gamma_{BR}). \quad (4)$$

After R successfully decodes $\mathbf{X}_M$ and $\mathbf{X}_B$, it generates N_R additional parity check bits based on the $N_M + N_B$ received bits from the previous transmission. Then, R broadcasts these N_R parity check bits as a vector of $\mathbf{X}_R$ to both M and B in the third phase. The vectors $\mathbf{X}_M$, $\mathbf{X}_B$ and $\mathbf{X}_R$ form a structure of distributed LDPC codes, where the relationship between them can be illustrated using the Tanner graph in Fig. 2, and the corresponding parity check matrix for the codes is given by

$$H = \begin{pmatrix} H_M & 0 & 0 \\ 0 & 0 & H_B \\ H_{1R} & H_{2R} & H_{3R}, \end{pmatrix} \quad (5)$$

where H_M and H_B are the parity check matrices used by R to decode $\mathbf{X}_M$ and $\mathbf{X}_B$, respectively. After obtaining $\mathbf{X}_M$ and $\mathbf{X}_B$, R uses H_{1R}, H_{2R} and H_{3R} to generate the additional N_R parity check bits.

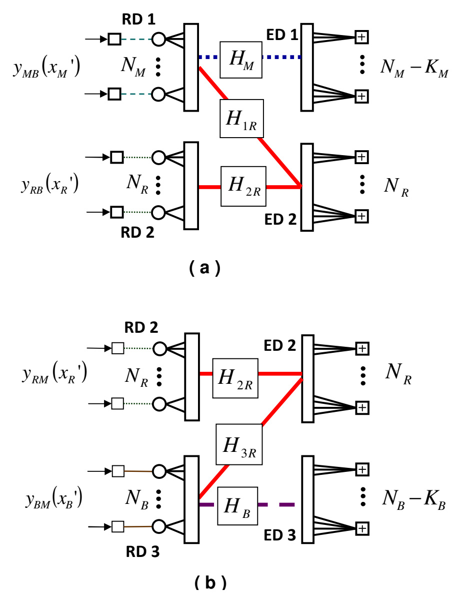

Fig. 3. (a) The Tanner graph to decode $\mathbf{X}_M$ at the base station in the uplink transmission. (b) The Tanner graph to decode $\mathbf{X}_B$ at the mobile station in the downlink transmission. The notation ED*i* is the edge degree of type *i* connecting the variable and check nodes, while RD*j* is the received degree connecting the variable nodes to the received symbols transmitted through channel *j*.

B. Channel decoding

Now, we describe the decoding process of $\mathbf{X}_M$, $\mathbf{X}_B$ and $\mathbf{X}_R$ at R, M and B, respectively. Since the transmissions are orthogonalized in time, the decoding of $\mathbf{X}_M$ and $\mathbf{X}_B$ at R is performed separately using the submatrix H_M and H_B. To ensure R can successfully decode $\mathbf{X}_M$ and $\mathbf{X}_B$, H_M and H_B must be designed so that (3) and (4) are satisfied.

The decoding procedure at B and M is slightly different from the decoding procedure at R. The base station (mobile station) only needs to obtain the messages transmitted by the mobile station (base station). To achieve better bit-error-rate (BER) performance, the decoding of $\mathbf{X}_M$ ($\mathbf{X}_B$) at the base station (mobile station) is performed with the help of N_R parity check bits from the relay. Since the base station (mobile station) already knows its own transmitted symbols, these symbols can be removed from the Tanner graph in Fig. 2 by updating the N_R parity check bits transmitted by R. Hence, the decoding of $\mathbf{X}_M$ ($\mathbf{X}_B$) at the base station (mobile station) is performed under belief propagation (BP) using the simplified Tanner graph in Fig. 3. The parity check matrices to decode $\mathbf{X}_M$ and $\mathbf{X}_B$ at the base and mobile stations, respectively, can be written as

$$H_{dec}^B = \begin{pmatrix} H_M & 0 \\ H_{1R} & H_{2R} \end{pmatrix}, \quad H_{dec}^M = \begin{pmatrix} 0 & H_B \\ H_{2R} & H_{3R} \end{pmatrix}.$$

The subcodes $\mathbf{X}_M$, or $\mathbf{X}_B$, must satisfy $N_M - K_M$, or $N_B - K_B$, zero parities (enforced by H_M or H_B), respectively, and N_R extra (presumably nonzero) parities provided by the relay. The corresponding rates for H_{dec}^B and H_{dec}^M are given by

$$R_{dec}^B = \frac{K_M}{N_M + N_R} = R_{MR} \cdot \left(\frac{T_M}{T_M + T_R}\right) \quad (6)$$

$$R_{dec}^M = \frac{K_B}{N_B + N_R} = R_{BR} \cdot \left(\frac{T_B}{T_B + T_R}\right). \quad (7)$$

IV. Code Design

Now, we explain the methodology to design the distributed LDPC codes introduced from the previous section. To design this code, we need to optimize the degree distribution for all decoders used in both uplink (i.e. H_M and H_{dec}^B) and downlink (i.e. H_B and H_{dec}^M) transmissions. Note that the structure of the decoders in both uplink and downlink directions is similar. Both H_{dec}^B or H_{dec}^M consist a sub parity check matrix of H_M or H_B, respectively, to decode the mother code ($\mathbf{X}_M$ and $\mathbf{X}_B$) at the relay. As a result, a similar methodology can be applied to design H_M and H_{dec}^B for the uplink transmission, and H_B and H_{dec}^M for the downlink transmission. To explain our proposed code design in detail, we discuss the design of H_M and H_{dec}^B at R_{MR} and R_{dec}^B, respectively, for the uplink transmission, i.e. the Tanner graph in Fig. 3(a).

Remark 1: For symmetric TD-TWRC, we only need to design the distributed codes in one transmission direction, e.g. H_M and H_{dec}^B for the uplink transmission. This is because $R_{MR} = R_{BR}$ and $R_{dec}^B = R_{dec}^M$ (i.e., $H_M = H_B$ and $H_{dec}^M = H_{dec}^B$). The optimized uplink codes can be directly applied for the downlink transmission.

The structure of distributed LDPC codes H_{dec}^B has two additional features. Firstly, there is a statistical distinction between the edges in the codeword, as not all edges can be connected between any two variable and check nodes (e.g. the $N_M - K_M$ check nodes can only be linked to the N_M variable nodes). Secondly, different segments of the received symbols at B are transmitted through different channels (N_M variables go through M-B channel and N_R variables go through R-B channel) and experience difference SNRs. These additional features can be represented using the general concept of irregular LDPC codes introduced by the MET-LDPC codes. The MET-LDPC codes' ensemble can be specified through the following two multinomials associated to the variable and check nodes [11]

$$\upsilon(\mathbf{r}, \mathbf{x}) = \sum \upsilon_{\mathbf{b},\mathbf{d}} \mathbf{r}^{\mathbf{b}} \mathbf{x}^{\mathbf{d}} \quad \text{and} \quad \mu(\mathbf{x}) = \sum \mu_{\mathbf{d}} \mathbf{x}^{\mathbf{d}}.$$

To explain these equations, we denote n_e as the number of edge types used in the graph's ensemble and n_τ as the number of different channels over which a bit may be transmitted. $\mathbf{d} = [d_1, ..., d_{n_e}]$ is the *edge degree vector* (EDV) of length n_e, and $\mathbf{b} = [b_0, ..., b_{n_\tau}]$ is the *received degree vector* (RDV) of length $n_\tau + 1$. The vector of variables is denoted by $\mathbf{x} = [x_1, ..., x_{n_e}]$, while $\mathbf{r} = [r_o, ..., r_{n_\tau}]$ denotes the vector of variables corresponding to the received distributions. Here, $\mathbf{x^d} = \prod_{i=1}^{n_e} x_i^{d_i}$ and $\mathbf{r^b} = \prod_{i=0}^{n_\tau} r_i^{b_i}$. Finally, $\upsilon_{\mathbf{b},\mathbf{d}}$ and $\mu_{\mathbf{d}}$ correspond to the percentage of variable nodes with type $(\mathbf{b}, \mathbf{d})$ and check nodes with type $(\mathbf{d})$ in the graph.

We represent the structure of distributed LDPC code H_{dec}^B using two types of edge degree ($n_e = 2$) and two types of received degree ($n_\tau = 2$), as shown in Fig. 3(a). The submatrix H_M that connects N_M variable nodes with $N_M - K_M$ check nodes are represented using the edge degree of type 1, while the edges connecting N_M (i.e., the submatrix H_{1R}) and N_R (i.e., the submatrix H_{1R}) variable nodes with N_R additional parity check nodes are represented using the edge degree of type 2. Since N_M and N_R received variables have been transmitted through the M-B and R-B channels, respectively, the edges connecting N_M and N_R variable nodes to the received symbols are represented using two different received degrees of type 1 and type 2, respectively. The multinomials for H_{dec}^B can be written as follows

$$\upsilon(\mathbf{r}, \mathbf{x}) = r_1 \sum_{i>0}^{d_{v,1}} \sum_{j=0}^{d_{v,2}} \upsilon_{[0,1,0],[i,j]} x_1^i x_2^j + r_2 \sum_{j>0}^{d_{v,2}} \upsilon_{[0,0,1],[0,j]} x_2^j \quad (8)$$

$$\mu(\mathbf{x}) = \sum_{i>0}^{d_{c,1}} \mu_{[i,0]} x_1^i + \sum_{j>0}^{d_{c,2}} \mu_{[0,j]} x_2^j \quad (9)$$

where r_1 and r_2 denote the N_M and N_R received variables associated with the received symbols from the M-B and R-B channels, respectively. The EDV $\mathbf{d} = [i, j]$ represents two types of edge degree, with i and j denoting the variable or check node's degrees (sockets) of type 1 and type 2, respectively.

Now, the design problem is to find the optimum ensemble of MET-LDPC codes given in (8) and (9) that achieves the rate of R_{dec}^B in (6). This optimization is executed in two steps. In the first step, the code design begins with optimizing the ensemble of H_M at the rate of R_{MR} in (3) for the M-R channel. H_M can be designed using a standard irregular LDPC code's optimization method [12] as it is only represented via one edge type (edge degree of type 1). The optimized node perspective degree distribution pair of a standard irregular LDPC code consists of the polynomials $\mathring{\lambda}(x) = \sum_{i>0}^{d_{v,1}} \mathring{\lambda}_i x^{i-1}$

and $\mathring{\rho}(x) = \sum_{i>0}^{d_{v,1}} \mathring{\rho}_i x^{i-1}$, where the coefficient of $\mathring{\lambda}_i$ and $\mathring{\rho}_i$ are non-negative real numbers satisfying $\sum_{i>0}^{d_{v,1}} \mathring{\lambda}_i = 1$ and $\sum_{i>0}^{d_{v,1}} \mathring{\rho}_i = 1$, respectively. Since N_M variable nodes represent a subcode inside the H_{dec}^B, the optimized $\mathring{\lambda}(x)$ and $\mathring{\rho}(x)$ polynomials of H_M can be represented using the MET-LDPC code's multinomials in (8) and (9) as

$$\upsilon(\mathbf{r},\mathbf{x}) = r_1 \sum_{i>0}^{d_{v,1}} \upsilon_{[0,1,0],[i,0]} x_1^i \quad \text{and} \quad \mu(\mathbf{x}) = \sum_{i>0}^{d_{c,1}} \mu_{[i,0]} x_1^i,$$

respectively, with $\sum_{i>0}^{d_{v,1}} \upsilon_{[0,1,0],[i,0]} = L_M$ and $\sum_{i>0}^{d_{c,1}} \mu_{[i,0]} = L_M \cdot (1 - R_{MR})$. Each non-negative real numbers of $\upsilon_{[0,1,0],[i,0]}$ and $\mu_{[i,0]}$ can be computed using

$$\upsilon_{[0,1,0],[i,0]} = L_M \cdot \mathring{\lambda}_i \tag{10}$$

$$\mu_{[i,0]} = L_M \cdot \mathring{\rho}_i \cdot (1 - R_{MR}). \tag{11}$$

Here, $L_M = T_M/(T_M + T_R)$ is the percentage of N_M variables in H_{dec}^B.

The second step is to design H_{dec}^B so that it achieves the rate of R_{dec}^B. The design of H_{dec}^B is performed by optimizing the ensemble of H_{1R} and H_{2R}, while fixing the optimized ensemble of H_M obtained from the previous optimization, i.e. the search for the optimum degree distribution of H_{dec}^B in (8) and (9) is only performed within the edge degree of type 2. The optimization setting for H_{dec}^B is different from the standard optimization of LDPC codes in point-to-point channels, as N_M and N_R variables are transmitted and received through M-B and R-B channels, respectively, and experience two different SNRs. Here, we define σ_{N_M} and σ_{N_R} as the noise thresholds for N_M and N_R variables, respectively. So, the corresponding received SNRs for M-B and R-B channels are $\gamma_{MB} = 1/\sigma_{N_M}^2$ and $\gamma_{RB} = 1/\sigma_{N_R}^2$. With this definition, the average noise threshold for the overall $N_M + N_R$ codeword is given by

$$\sigma_{avg} = \sqrt{\frac{1}{L_M \cdot \frac{1}{\sigma_{N_M}^2} + L_R \cdot \frac{1}{\sigma_{N_R}^2}}} \tag{12}$$

where $L_R = T_R/(T_M + T_R)$ is the percentage of N_R variables in H_{dec}^B. In this work, we optimize H_{dec}^B using differential evolution [13] by maximizing (12) under multi-edge type density evolution [11], subject to $\sigma_{N_M} \le \sigma_{MB_{lim}}$ and $\sigma_{N_R} \le \sigma_{RB_{lim}}$, where $\sigma_{MB_{lim}}$ and $\sigma_{RB_{lim}}$ are the theoretical limits for M-B and R-B channels, respectively. Below we outline the procedure to generate the set of type 2 edge multinomials of H_{1R} and H_{2R} to initialize the optimization process using differential evolution.

1) For each optimized coefficient $\upsilon_{[0,1,0],[L,0]}$ of the N_M variable nodes, with L type 1 sockets, we generate j type 2 sockets to obtain $\upsilon_{[0,1,0],[L,j]}$. Then, we also generate j type 2 sockets to obtain $\upsilon_{[0,0,1],[0,j]}$ for the N_R variable nodes. At this stage, we have successfully generated the variable node's multinomial in (8).
2) We compute the total number of type 2 edges (sockets) for the generated variable node's multinomial using
$$\upsilon_{x_2}(\mathbf{1},\mathbf{1}) = \frac{d}{d_{x_2}} \upsilon(\mathbf{r},\mathbf{x}). \tag{13}$$
3) The average value of the check node degrees for $[H_{1R}\ H_{2R}]$ can be calculated using
$$d_{c,ave} = \frac{\upsilon_{x_2}(\mathbf{1},\mathbf{1})}{L_R}. \tag{14}$$
4) We generate a concentrated type 2 edge multinomial for the check nodes. This multinomial is given by
$$\mu_{[0,d_{c,2}]} \cdot x_2^{d_{c,2}} + \mu_{[0,d_{c,2}-1]} \cdot x_2^{d_{c,2}-1} \tag{15}$$
where $d_{c,2} = \lceil d_{c,ave} \rceil$ and $\lceil \cdot \rceil$ denotes the ceiling function. The values of $\mu_{[0,d_{c,2}]}$ and $\mu_{[0,d_{c,2}-1]}$ are obtained by solving the following two equations
$$L_R = \mu_{[0,d_{c,2}]} + \mu_{[0,d_{c,2}-1]} \tag{16}$$
$$\upsilon_{x_2}(\mathbf{1},\mathbf{1}) = d_{c,2} \cdot \mu_{[0,d_{c,2}]} + (d_{c,2} - 1) \cdot \mu_{[0,d_{c,2}-1]}. \tag{17}$$
5) At the end of step 4, we have successfully generated the check node's multinomials in (9). The average noise threshold of the generated variable and check nodes' multinomials of H_{dec}^B can then be computed using density evolution.

After all multinomials in the initial set (population) are generated, the process of mutation, recombination and selection of the differential evolution algorithm are performed to obtain the optimum H_{dec}^B.

Remark 2: For asymmetric TD-TWRC (i.e. $H_M \neq H_B$ and $H_{dec}^M \neq H_{dec}^B$), we have to separately design H_B and H_{dec}^M for the downlink transmission after we designed H_M and H_{dec}^B for the uplink transmission. To design H_B and H_{dec}^M, the proposed two steps procedure is slightly modified. This is because H_{dec}^M shares the same sub-matrix of H_{2R} in H_{dec}^B (for the shared N_R variables generated by the relay), which has already been optimized when H_{dec}^B is designed for the uplink transmission. So, after H_B is designed for the B-R channel in the first optimization step, designing H_{dec}^M in the second optimization step is only performed by optimizing the ensemble of H_{3R} for the N_B variables, while fixing the optimized ensemble of H_B and H_{2R} obtained from the previous optimization.

V. Numerical results

We evaluate our proposed methodology by designing the uplink distributed LDPC code for a particular symmetric TD-TWRC, where the BAWGN capacities for each link are given as follows, $C(\gamma_{MR}) = C(\gamma_{BR}) = 0.8$ and $C(\gamma_{MB}) = 0.4$. Applying (2), the optimal values of time sharing parameters that maximize the uplink transmission rate are $T_M = T_B = 0.4$ and $T_R = 0.2$. The designed rates for the parity check matrices H_M and H_{dec}^B are $R_{MR} = 0.8$ and $R_{dec}^B = 0.5333$, respectively.

The code design starts with optimizing H_M at $R_{MR} = 0.8$ using a standard optimization method for single link LDPC codes. The optimized degree distribution for H_M is obtained from [12], where the corresponding LDPC code associated with $\mathbf{X}_M$ performs asymptotically at 0.13382 dB from the theoretical limit. Then, the optimization of H_{dec}^B is performed by searching the ensemble of H_{1R} and H_{2R} (the edge degree

RDV			EDV						
Type 0	Type 1	Type 2	$\upsilon_{[i,j]}$	Type 1	Type 2		$\mu_{[i,j]}$	Type 1	Type 2
0	1	0	0.09652	2	0		0.13333	20	0
0	1	0	0.04710	2	14		0.08388	0	7
0	1	0	0.11899	2	2		0.24946	0	8
0	1	0	0.04675	3	3				
0	1	0	0.066181	3	0				
0	1	0	0.12966	3	1				
0	1	0	0.06474	6	6				
0	1	0	0.01534	6	1				
0	1	0	0.00869	7	6				
0	1	0	0.02494	12	6				
0	1	0	0.04776	12	3				
0	0	1	0.33333	0	2				

R_{MR} , R^B_{dec}	0.8 , 0.5333
σ^*_{MR} , σ^*_{avg} ($\sigma^*_{N_M}$, $\sigma^*_{N_R}$)	0.61553 , 0.84208 (1.132, 0.612)
gap_{MR} , gap_{avg}	0.13382 dB , 0.16324 dB

TABLE I

THE OPTIMIZED MULTINOMIALS FOR H^B_{dec} DESIGNED AT ($R_{MR} = 0.8$, $R^B_{dec} = 0.5333$).

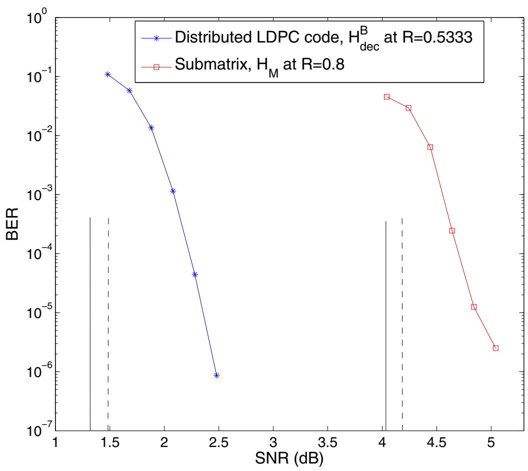

Fig. 4. BER performances for H_M and H^B_{dec}. The solid and dotted lines represent the theoretical limit and the asymptotic threshold for the code at the correspondence design rates.

of type 2), while fixing the optimized H_M (the edge degree of type 1). The optimized degree distribution for H^B_{dec} is given by the node-perspective multinomial representation in Table I. The optimized H^B_{dec} performs asymptotically within 0.16324 dB from the theoretical limit, i.e. the code achieves the thresholds of $\sigma^*_{N_M} = 1.132$ for N_M variables transmitted through the M-B link, and $\sigma^*_{N_R} = 0.612$ for N_R variables transmitted through the R-B link. We then simulate the finite-length performances for the code with block length of $N_M = 8000$ bits, and $N_M + N_R = 12000$ bits for H_M and H^B_{dec}, respectively, and plot the BER curves in Fig. 4. At an error probability of 10^{-5}, the code performs around 0.8 dB and 1 dB away from the theoretical limit for H_M and H^B_{dec}, respectively.

VI. CONCLUSION

We have extended the general concept of irregular LDPC codes, captured by MET-LDPC codes, to construct the distributed LDPC codes for symmetric TD-TWRC. A new design methodology has been proposed, where we transform the design of distributed LPDC codes into a problem of optimizing MET-LDPC codes. In order to optimize the codes under density evolution, we formulate the average threshold for the proposed code design. This is because the received bits within a single distributed codeword have been transmitted through different channels and experience different SNRs.

REFERENCES

[1] R. Ahlswede, N. Cai, S-Y. R. Li, and R.W. Yeung, "Network information flow," *IEEE Trans. Inform. Theory*, vol. 46, no. 4, pp. 1204–1216, July. 2000.

[2] B. Rankov, and A. Wittheben, "Achievable rate regions for the two-way relay channel," *in Proc. IEEE Int. Symp. Inf. Theory*, pp. 1668–1672, Jul. 2006.

[3] S.J. Kim, P. Mitran and V. Tarokh, "Performance bound for bidirectional coded cooperation protocols," *IEEE Trans. Inform. Theory*, vol. 54, no. 11,, Nov. 2008.

[4] A.B. Saleh, C. Hausl and R. Kotter, "Outage behaviour of bidirectional half-duplex relaying schemes," *IEEE Inform. Theory Workshop (ITW)*, Oct. 2009.

[5] C. Hausl and J. Hagenauer, "Iterative network and channel coding for the two-way relay channel," *IEEE International Conference on Communications (ICC)*, pp. 1568–1573, June 2006.

[6] J. Hou, C. Hausl and R. Kotter, "Distributed turbo coding schemes for asymmetric two way relay communication,"*IEEE Intl. Workshop on turbo codes and related topics (ICC)*, pp. 237–242, Sept. 2008.

[7] T. J. Richardson and R. L. Urbanke, "The capacity of low-density parity-check codes under message passing decoding," *IEEE Trans. Inform. Theory*, vol. 47, no. 2, pp. 599–618, Feb. 2001.

[8] P. Razaghi and W. Yu, "Bilayer LDPC codes for decode-and-forward in relay channels," *IEEE Trans. Inform. Theory*, vol. 53, no. 10, pp. 3723–3739, Oct. 2007.

[9] M.R. Yazdani and A.H. Banihashemi, "On construction of Rate-Compatible Low-Density Parity-Check Codes," *IEEE Commun. Letter*, vol. 8, no. 3,, March 2004.

[10] C. Hausl, "*Joint Network-Channel coding for wireless relay networks*," Dissertation, Technical University of Munich, Nov. 2008.

[11] T. Richardson and R. Urbanke, Multi-Edge Type LDPC Codes [Online]. Available: http://lthcwww.epfl.ch/papers/multiedge.ps

[12] "A fast and accurate degree distribution optimizer for ldpc code ensembles", Available: http://ipgdemos.epfl.ch/ldpcopt/

[13] K. Price and R. Storn, "Differential evolution - a simple and efficient heuristic for global optimization over continuous spaces," *J. Global Optimiz.*, vol. 11, pp. 341–359, 1997.